

Research Article

Infiltration Behaviour of Polymer-Modified Porous Concrete and Porous Asphalt Surfaces Used in SuDS Techniques[†]

Luis A. Sañudo-Fontaneda^{1,*}, Jorge Rodriguez-Hernandez¹, Miguel A. Calzada-Pérez², and Daniel Castro-Fresno¹

¹ Construction Technology Applied Research Group (GITECO), Escuela Técnica Superior de Ingenieros de Caminos, Canales y Puertos, Universidad de Cantabria, Santander, Spain

² Highways Research Group (GCS). Escuela Técnica Superior de Ingenieros de Caminos, Canales y Puertos, Universidad de Cantabria, Santander, Spain

Correspondence: L. A. Sañudo-Fontaneda, Construction Technology Applied Research Group (GITECO), Escuela Técnica Superior de Ingenieros de Caminos, Canales y Puertos, Universidad de Cantabria. Avenida de los Castros s/n, 39005 Santander, Spain

E-mail: sanudola@unican.es

Running title: Infiltration Behaviour of Porous Surfaces Used in SUDS

[†]This article has been accepted for publication and undergone full peer review but has not been through the copyediting, typesetting, pagination and proofreading process, which may lead to differences between this version and the Version of Record. Please cite this article as an 'Accepted Article', doi: [10.1002/clen.201300156].

© 2013 WILEY-VCH Verlag GmbH & Co. KGaA, Weinheim
Received: March 1, 2013 / Revised: May 17, 2013 / Accepted: June 7, 2013

ABBREVIATIONS: **BMP**, best management practice; **CF**, Cantabrian fixed; **C_{IR}**, cumulative infiltration rate; **EPA**, (United States) Environmental Protection Agency; **ICBP**, interlocking concrete blocks pavement; **PA**, porous asphalt; **PMPC**, polymer-modified porous concrete; **R_R**, residual runoff; **R_{SL}**, runoff surface length; **S_S**, surface slope; **SuDS**; sustainable drainage system

Keywords: clogging; geotextiles; regression models; stormwater management

Abstract

Permeable pavements are one of the world's most widely applied techniques for source control in sustainable drainage systems. Porous concrete (PC) and porous asphalt (PA) are two of the most studied surfaces in terms of runoff reduction. Nevertheless, previous research has highlighted a lack of a comprehensive laboratory methodology for the analysis of the topographical variables, runoff surface length (R_{SL}) and surface slope (S_S), and their impact on the infiltration behaviour of these porous surfaces. This research paper analyses the infiltration performance of polymer-modified PC and PA-16 for 0, 3, 5, 7 and 10% slope on newly built and clogged surfaces, using an improved version of the Cantabrian fixed (CF) infiltrometer and LCS permeameter, enabling comparison of the infiltration behaviour. This laboratory methodology has proved to be well suited to the study of the infiltration behaviour of porous surfaces and also to the quantification of their infiltration capacity reduction due to clogging. As main results, this paper presents regression models with high R^2 obtained with a confidence level of 95%, based on R_{SL} and S_S variables, corresponding to each porous surface and clogging level.

1. Introduction

Permeable pavements are the most widely used technique for source control in sustainable drainage systems (SuDS) to mitigate flooding [1]. Permeable pavements can occupy large urban areas, especially through their use in car parks [2], reducing runoff and diffuse pollution by retaining pollutants [3]. Porous pavements such as porous concrete (PC) and porous asphalt (PA) have been widely used in car parks to increase the infiltration capacity of pervious pavements during recent years. For instance, the EPA considers PC surfaces to be one of the best management practices (BMPs) due to their high percentage of voids and their additional properties (resistance improvement, noise and heat reduction) compared with other permeable surfaces [4]. Recently studies have demonstrated that polymer-modified PC (PMPC) presents better fatigue behaviour [5] and infiltration capacity than standard PC [6].

A typical permeable paving structure has a permeable surface of porous material or impervious material with joints, a base layer made of aggregates, a separation and a geotextile filtration layer and a sub-base made of stone (Fig. 1). Nowadays, the most widely used permeable surfaces are made of interlocking concrete blocks pavement (ICBP) in the case of impervious materials in which the infiltration occurs through the joints and PC and PA porous surfaces where case infiltration occurs through their void structure. A standard permeable paving structure made of PC or PA porous surfaces is shown in Fig. 1.

Loss of permeability due to clogging is the main problem of PC and PA surfaces, highlighted by research all over the world [7]. Clogging problems are due to long-term deposition of sediments carried by surface runoff or short-term events such as catastrophic flooding [8]. In spite of the fact that there were many studies in which the impact of clogging on permeable surfaces had been analysed, Lucke et al. [9] and Sañudo-Fontaneda et al. [10] pointed out that not all variables regarding topography had been studied (surface slope and flow distance) and, using ICBP surfaces, they demonstrated the significant impact of these variables in the general analysis of clogging. Their study not only took into account the influence of surface runoff from adjacent impervious surfaces, which was commonplace in research, but also the influence of direct rainfall.

The main aim of this paper is to translate this methodology toward porous surfaces in order to obtain a common methodology for the analysis of the infiltration behaviour of permeable pavements. Moreover, specific objectives, divided into two main aspects, will be addressed. The infiltration behaviour of PMPC and PA-16 (PA with 16 mm of maximum aggregates size) will be analysed based on the topographic variables runoff surface length (R_{SL}) and surface slope (S_s), using the CF infiltrometer with different levels of clogging. Two regression models, which simulate both newly built and clogged surfaces, will be proposed to explain the infiltration process. Furthermore, the reduction of the infiltration capacity due to clogging in porous surfaces and geotextiles will be evaluated, and the real impact of clogging on the appearance of residual runoff on porous surfaces will be assessed.

2. Materials and Methods

2.1. Materials

The materials used to simulate a permeable pavement structure in this research were PMPC and PA-16 [11] as porous surface, limestone aggregates as base layer and geotextile as separation and filtration layer (Fig. 1). No sub-base layer was studied in this research because its permeability is usually higher than the other layers and it is not the limiting factor.

The PMPC layer was 100 mm thick, with 18 and 27 MPa of compressive strength measured according to European Standards [12]-[14] after 7 and 28 days, respectively, with 25% voids, and 1778 kg/m³ apparent density obtained following the European Standards [15].

Another porous surface layer 100 mm thick of PA-16 with 2050 kg/m³ apparent density and 23.45% voids was also used. It had a particle size distribution of the ophite agglomerate.

A 50-mm thick base layer of limestone aggregate with a particle size of 4-6 mm, 1.354 g/cm³ apparent density and 50% voids was used as the permeable paving structure.

Finally, one polyester nonwoven geotextile was used as the bottom layer with the characteristics shown in Table 1. The geotextile has two main functions: filtration of water and separation of the base and sub-base layers.

The sediment used to clog porous PMPC and PA-16 surfaces in order to simulate a catastrophic scenario of flooding was limestone silt with particle size distribution shown in Fig. 2. The difference between particle size distribution of sediments used to clog the ICBP surface [16], and the distribution used to clog PMPC and PA-16 in this research can also be observed. The distribution of the latter was based on studies

carried out on PC by [17] and studies carried out on PA by [7] (Fig. 2). A high percentage of fine sediments due to previous researches [8] that demonstrated a high decrease in the infiltration rates of PC with an increasing percentage of fine sediments. Davies et al. demonstrated that organic matter is the cause of a major decrease in the infiltration capacity of ICBP [16]. Therefore, 14% of organic matter was introduced, through the use of sawdust, in the range of fines up to 0.5mm of particle size in order to decrease the infiltration capacity of PMPC and PA-16.

2.2. Experimental methodology

2.2.1. Analysis of the infiltration behaviour

The infiltration behaviour of PMPC and PA-16 surfaces was analysed using the CF infiltrometer of the University of Cantabria [18] with the modifications introduced by [10] in order to achieve more accurate results. The CF infiltrometer is an experimental laboratory device that enables the simulation of rainfall intensities in the range of 10-150 mm/h for any storm event duration and surface slopes between 0 and 10% under controlled laboratory conditions of 16°C and 75% of humidity (Fig. 3).

The variables studied in this research were chosen after an analysis of the most influential variables in previous infiltration studies. The independent variables were the runoff surface length (R_{SL}) which is the distance (cm) measured from the top part of the porous surface specimen, and surface slope (S_s) (%) (Fig. 3). The dependent variable was the cumulative infiltration rate (C_{IR}), which is the cumulative percentage of infiltration rate, measured in each water infiltration chamber (Fig. 3).

An extreme rainfall of 60 mm/h, corresponding to a 50-year return period with duration of 30 min was simulated over three $50 \times 50 \text{ cm}^2$ test specimens of PMPC and another three test pieces of PA-16 surfaces, and slopes of 0, 3, 5, 7 and 10%, following the same procedure described in [10] for ICBP surfaces. Two different scenarios of clogging were tested on the CF infiltrometer for each test piece in order to simulate two extreme periods of the operational life of porous surfaces, corresponding to an initial, newly built surface in which the porous surface is free of sediments, and a clogged surface, simulating their behaviour after a catastrophic event related to a massive pouring of sediments from a construction site [7]. The latter clogging level was simulated using sediments described in Section 2.1, representing the amount of sediments necessary to clog a porous surface, according to [16]. The sediments were applied following the methodology demonstrated by [7] for PA surfaces with slight hand-compaction. Finally, a light brushing was used to simulate sweeping machines that clean sediments from urban surfaces in Spain, in order to analyse the possible recovery of permeability after this type of maintenance.

Previous studies highlighted that an initial period of 10 min was necessary to achieve the steady-state stage [16], and then the measuring stage used in the CF infiltrometer lasted 20 min, as in [7], collecting infiltrated and residual runoff water in the chambers prepared for this purpose (Fig. 3). Calibration tests carried out on both porous surfaces in this research highlighted that just 3 min were necessary to achieve steady state conditions. In each case, all measurements were recorded over 20 min of time after 10 initial min, maintaining the same procedure.

Darcy's law can be applied to the infiltration process which takes place during the steady-state stage on

Accepted Preprint

PMPC and PA-16 porous surfaces, and base layer of aggregates, according to previous researchers such as [19], [20], assuming that the infiltration process of a non-saturated porous media is governed by the Navier-Stokes equations. The theoretical hydraulic phenomena described in this test pointed out that the hydraulic conductivity always facing the rainfall intensity simulated in each test undertaken, using the CF infiltrometer, as was demonstrated by Sañudo-Fontaneda et al. [10].

2.2.2. Reduction of the infiltration capacity

The reduction of the infiltration capacity was measured through the difference between permeabilities measured on porous surfaces and geotextiles in both the initial scenario of clogging with a newly built surface without sediments and in the final scenario of clogged surface without maintenance. Clogged scenario was achieved by adding 2000 g/m² of the sediments (Fig. 2) in both porous surfaces in contrast to the research of Rodriguez-Hernandez et al. [7]. The LCS permeameter, which is a falling-head permeameter for PA surfaces, and the equipment of water permeability normal to the plane, without load, LAGUC E-003 (ENSA 3HL8-200) (Fig. 4) were used based on European Standards [15]. Charbeneau et al. demonstrated that the LCS permeameter can also be used on PC surfaces to measure their permeability [22].

LCS was applied at the midpoint of both sides of each test piece to calculate the average permeability in the case of a newly built surface scenario with clogging. However, in the case of the clogging scenario, two different zones could be observed due to the influence of the drops with a kinetic energy of 5.6×10^{-4} J and 3.5 mm diameter from the direct rainfall simulator which has 5 lines of 15 adjustable drippers (0-40 L/h) each. The drops take away part of the sediments that clog the surface in the zone where the drops hit the surface during the CF infiltrometer test. Hence, two different zones can be observed; a clogged zone where the drops did not touch the surface and a less clogged zone where the drops contacted the surface. 24 points of measurement were taken with the LCS permeameter (12 in each zone) in order to check the permeability reduction over both porous surfaces and the possible impact of the drops in producing different zones of permeability in the same test piece.

A comparative analysis is presented in this paper between the reduction of permeability and the influence of the type of porous surface, clogging scenario and surface slope on the residual runoff (R_R) measured in the infiltration behaviour test (Fig. 3). Finally, the behaviour of the sediments will be analysed through their migration from the surface toward the geotextile layer, by determining mass per unit area based on the European Standard [23].

3. RESULTS AND DISCUSSION

3.1. Infiltration behaviour test

All regression models were obtained under the laboratory conditions detailed previously for a 95% confidence level, fulfilling the statistical criteria of analysis of co-linearity, independence of observations, normality of the standardised residues of the dependent variable, and homocedasticity (Table 2, Fig. 5). Sample size was always 75 for each clogging level and porous surface.

R_{SL} is the most influential variable in all models as can be seen in Table 2, showing a positive relation

with C_{IR} . S_S also has an important impact on the model and its relation is negative, C_{IR} decreasing when S_S increases. The constant is not significant in all models, registering a p -value >0.05 in all cases. This point and high R^2 together make these regression models a good predictor of the infiltration behaviour of PMPC and PA-16 surfaces.

3.2. Reduction of the infiltration capacity

The LCS test applied to both porous surfaces showed an average difference of permeability in the newly built scenario of 40% between PMPC (0.020 m/s) and PA-16 (0.012 m/s) surfaces and 58.33% after clogging (Table 3). The average reduction in the permeability after clogging was 33.05% for PMPC, while the reduction for PA-16 was 64.16%, being much more influential in the latter case (Table 3), using the same sediments and clogging procedure. Infiltration capacity for PMPC after clogging was 0.012 mm/s, being nearly 2.4 times higher than PA-16's infiltration capacity (0.005 mm/s) at the same clogging level. The difference in permeability between clogged zones and less clogged zones in the same test piece, found in both surfaces after clogging, was 44.97% for the PMPS surface and 42.50% for the PA-16 surface. It was noted that drops took away part of the sediments used to clog both porous surfaces.

This high reduction in permeability only caused a slight increase in the residual runoff from 7% surface slope, always $<1\%$ for slopes up to 5% in both porous surfaces. Therefore, both surfaces still continue to infiltrate $>90\%$ of the total direct rainfall and surface runoff from adjacent impervious surfaces in the first 50 cm of the porous surface, which is the surface tested in the CF infiltrometer.

A statistical analysis of the bivariate correlations was undertaken in order to study the impact on residual runoff of the type of porous surface, clogging level (newly built surface and clogged surface) and surface slope. It was established that R_R has a positive relation with the type of surface, being higher for the PMPC than the PA-16 surface. According to the Spearman coefficients with p -value >0.05 shown in Table 4, it can also be observed that the clogging level is not linearly related with R_R under this procedure of adding sediments. However, a highly linear relation exists between S_S and R_R : an increasing R_R when S_S increases (Fig. 6).

The geotextile used in this research had a high permeability of 155.10 mm/s in the case of the newly built surface. However, permeabilities of 154.42 and 155.50 mm/s were obtained after clogging in PMPS and PA-16 surfaces, respectively. In addition, the average mass measured after clogging was 188.60 g/m² in the case of PMPC and 170 g/m² in the case of PA-16 surface. Hence, 38.60 and 20 g of sediments were retained by the geotextile per m², corresponding to 7.72 and 4% of the total amount of sediments used to clog PMPC and PA-16 porous surfaces, respectively. In spite of the important amount of sediments trapped in the geotextile, permeability did not decrease. This fact is explained by the degradation observed in the geotextile, producing local spaces in which the local permeability was much higher than the permeability of a newly built surface. Moreover, the majority of the sediments used to clog the porous surfaces were retained by upper layers such as the surface layer and the base layer, especially the former (Fig. 7), confirming previous studies by [24].

Maintenance used in this research was able to remove an average amount of sediments of 44.50 g from both porous surfaces (8.90% of the total amount of sediments used to clog the two surfaces). However, it

should also be said that the kind of maintenance used in this research does not lead to a recovery in the infiltration capacity of porous surfaces as in the case of ICBP [9]. This finding tries to emphasize previous conclusions obtained by Ferguson [25] who had been demonstrated that vacuuming was more effective than sweeping at maintaining or restoring infiltration in porous surfaces.

4. CONCLUDING REMARKS

After the analysis of the infiltration behaviour of PMPC and PA-16 in the laboratory, with the CF infiltrometer, regression models were obtained based on the topographical variables in newly built and clogged surfaces, with a confidence level of 95%, and with R^2 values >0.85 .

The most influential topographical variable in the regression models was always R_{SL} compared to S_s .

From this study of the reduction of the infiltration capacity with the LCS in laboratory, it is concluded that PMPC surfaces had a greater infiltration capacity (40%) than PA-16 surfaces, in the case of newly built surfaces. Under the methodology used for clogging in this paper, the reduction of the infiltration capacity for PMPC surfaces was 33.05%, while reduction for PA-16 was 64.16% under the methodology used in this paper.

However, these reductions of the infiltration capacity has a slight impact on residual runoff, as can be observed in the values of infiltration $>90\%$ of the total either direct rainfall and surface runoff from adjacent impervious surfaces in all clogging scenarios, with the CF infiltrometer.

In future, field tests will be developed to validate the regression models obtained in the laboratory.

ACKNOWLEDGEMENTS

This study was funded by the Spanish Ministry of Economy and Competitiveness through the research project BIA2009-08272. The authors also want to thank the research groups GCS and GITECO, and the laboratories LAGUC and SUDSlab of the University of Cantabria, and the companies SIEC SA, SENOR SA and DANOSA for their collaboration. Luis A. Sañudo-Fontaneda also thanks Ministry of Economy and Competitiveness for the FPI fellowship.

The authors have declared no conflict of interest.

5. REFERENCES

- [1] B. O. Brattebo, D. B. Booth, Long-term stormwater quantity and quality performance of permeable pavement systems, *Water Res.* 2003, 37, 4369-76.
- [2] X. Shu, B. Huang, H. Wu, Q. Dong, E. G. Burdette, Performance comparison of laboratory and field produced pervious concrete mixtures, *Constr. Build. Mater.* 2011, 25 (8), 3187-3192.
- [3] B. T. Rushton, Low-impact parking lot design reduces runoff and pollutant loads, *J. Water Resour. Plann. Manage.* 2001, 127 (3), 172-179.
- [4] A. Golroo, S. L. Tighe, Alternative modeling framework for pervious concrete pavement condition analysis, *Constr. Build. Mater.* 2011, 25 (10), 4043-4051.
- [5] M. Á. Pindado, A. Aguado, A. Josa, Fatigue behavior of polymer-modified porous concretes, *Cem. Concr. Res.* 1999, 29 (7), 1077-1083.
- [6] H. B. Kim, K.-H. Lee, An innovative rehabilitation approach for the bridge deck pavement, in *Conference Proceedings of the GeoHunan International Conference - New Technologies in Construction and Rehabilitation of Portland Cement Concrete Pavement and Bridge Deck Pavement*, American Society of Civil Engineers, Red Hook, NY **2009**, pp. 19-27.
- [7] J. Rodriguez-Hernandez, D. Castro-Fresno, A. H. Fernández-Barrera, Á. Vega-Zamanillo, Characterization of Infiltration Capacity of Permeable Pavements with Porous Asphalt Surface Using Cantabrian Fixed Infiltrometer, *J. Hydrol. Eng.* 2012, 17 (5), 597-603.
- [8] L. M. Haselbach, Potential for clay clogging of pervious concrete under extreme conditions, *J. Hydrol. Eng.* 2010, 15 (1), 67-69.
- [9] T. Lucke, J. Rodriguez-Hernandez, L. A. Sañudo-Fontaneda, S. Beecham, The influence of slope on the infiltration performance of permeable pavements, *XXXIII Convegno Nazionale di Idraulica e Costruzioni Idrauliche*, Brescia, Italy **2012**, pp. 1-10.
- [10] L. A. Sañudo-Fontaneda, J. Rodriguez-Hernandez, A. Vega-Zamanillo, D. Castro-Fresno, Laboratory analysis of the infiltration capacity of Interlocking Concrete Block Pavements in car parks, *Water Sci. Technol.* 2013, 67 (3), 675-681.
- [11] G. Bustos, E. Pérez, *Pliego de prescripciones técnicas generales para obras de carreteras y puentes*, Ediciones LITEAM, Madrid **2007**.
- [12] European Standard EN 12390-1, *Testing hardened concrete - Part 1: Shape, dimensions and other requirements for specimens and moulds*, European Committee for Standardization, Brussels **2012**.
- [13] European Standard EN 12390-2, *Testing hardened concrete - Part 2: Making and curing specimens for strength tests*, European Committee for Standardization, Brussels **2009**.
- [14] European Standard EN 12390-3, *Testing hardened concrete - Part 3: Compressive strength of test specimens*, European Committee for Standardization, Brussels **2009**.
- [15] European Standard EN 12697-40, *Bituminous mixtures - Test methods for hot mix asphalt - Part 40: In situ drainability*, European Committee for Standardization, Brussels **2006**.
- [16] J. W. Davies, C. J. Pratt, M. A. Scott, Laboratory study of permeable pavement system to support hydraulic modelling, in *Conference Proceedings of the 9th International Conference on Urban Drainage (9ICUD)*, Portland, Oregon **2002**, pp. 1-9.

- [17] S. A. Tan, T. F. Fwa, V. Y. K. Guwe, Laboratory Measurements and Analysis of Clogging Mechanism of Porous Asphalt Mixes, *J. Test. Eval.* 2000, 28 (3), 207-216.
- [18] J. Rodríguez, D. Castro, M. A. Calzada, J. W. Davies, Pervious Pavement Research in Spain: Structural and Hydraulic issues, in *Conference Proceedings of the 10th International Conference on Urban Drainage (10ICUD)*, Copenhagen, Denmark **2005**, pp. 1-8.
- [19] J. Sansalone, X. Kuang, V. Ranieri, Permeable pavement as a hydraulic and filtration interface for urban drainage, *J. Irrig. Drain. Eng.* 2008, 134 (5), 666–674.
- [20] R. J. Charbeneau, J. B. Klenzendorf, M. E. Barrett, Methodology for determining laboratory and in situ hydraulic conductivity of asphalt permeable friction course, *J. Hydraul. Eng.* 2011, 137 (1), 15–22.
- [21] European Standard EN ISO 11058, *Geotextiles and geotextile-related products - Determination of water permeability characteristics normal to the plane, without load*, European Committee for Standardization, Brussels **2010**.
- [22] A. H. Fernández-Barrera, D. Castro-Fresno, J. Rodríguez-Hernández, M. A. Calzada-Pérez, Infiltration capacity assessment of urban pavements using the LCS permeameter and the CP infiltrometer, *J. Irrig. Drain. Eng.* 2008, 134 (5), 659-665.
- [23] European Standard EN ISO 9864, *Geosynthetics. Determination of mass per area unit*, European Committee for Standardization, Brussels **2005**.
- [24] T. Lucke, S. Beecham, Field Investigation of Clogging in a Permeable Pavement System, *J. Build. Res. Inf.* 2011, 39 (6), 603-615.
- [25] B. K. Ferguson, Porous pavements, in *Integrative Studies in Water Management and Land Development* (Ed.: R. L. France), 6th Series, CRC Press, Boca Raton **2005**.

Figure 1. Schematic cross section of a standard permeable paving structure made of PC or PA.

Figure 2. Size distribution of the sediments used to clog the PMPC and PA-16 surfaces in comparison with the sediments used to clog ICBP surfaces.

Figure 3. Scheme of the CF infiltrometer and the variables measured on the infiltration behaviour test.

Figure 4. LCS permeameter and the equipment of water permeability normal to the plane, without load LAGUC E-003 (ENSA 3HL8-200) based on European standards.

Figure 5. Relationship between C_{IR} , R_{SL} and S_S in all regression models obtained for PMPC and PA-16 surfaces.

Figure 6. Relationship between S_S and R_R .

Figure 7. Sediments clogging PA-16 surface, especially focused on their migration toward the geotextile.

Table 1. Main characteristics of the geotextile, DANOFELT PY 150.

Geotextile DANOFELT PY 150				
Average mass (g/m ²)	Longitudinal tensile strength (KN/m)	Transverse tensile strength (KN/m)	Thickness under 2 kPa pressure (mm)	Opening size (μm)
UNE EN 965	UNE EN ISO 10319	UNE EN ISO 10319	UNE EN 964	UNE EN ISO 12956
150	1.2	1.2	1.90	100

Table 2. Regression models obtained for PMPC and PA-16 surfaces in each clogging levels.

Porous surface		Regression model	R^2	Student's t -test		
				C	R_{SL}	S_S
PMPC	Newly built	$C_{IR} = 6.262 + 2.074 R_{SL} - 3.774 S$	0.85	1.438	18.637	-8.168
PA-16	Newly built	$C_{IR} = 8.868 + 2.044 R_{SL} - 4.406 S$	0.87	1.963	17.805	-11.302
PMPC	Clogged	$C_{IR} = 7.741 + 2.094 R_{SL} - 4.158 S$	0.88	1.994	21.164	-10.007
PA-16	Clogged	$C_{IR}^{1/2} = 1.324 + 0.213 R_{SL} - 0.436 S$	0.89	3.565	22.406	-11.057

Table 3. Permeability values of the LCS tests in the three test pieces of PMPC and PA-16 after clogging and percentage of permeability reduction in comparison with values of the newly built surface.

Clogged surface		PMPC			PA-16		
Test piece	Zone	Average permeability (m/s)	Reduction (%)	Average permeability (m/s)	Reduction (%)		
1	Clogged	0.009	13.33	0.005	53.85		
	Less clogged	0.017		0.008			
2	Clogged	0.008	40.00	0.003	63.64		
	Less clogged	0.015		0.005			
3	Clogged	0.010	45.83	0.002	75.00		
	Less clogged	0.017		0.004			

Table 4. Spearman's Rho coefficients obtained in the statistical analysis of the bivariate correlation.

		Residual runoff (R_R)	Type of porous surface	Surface slope	Clogging level
Residual runoff (R_R)	Correlation coefficient	1.000	-0.481**	0.660**	0.227
	Significance (bilateral)	—	0.000	0.000	0.081
** Correlation is significant at level 0.01 (bilateral).					

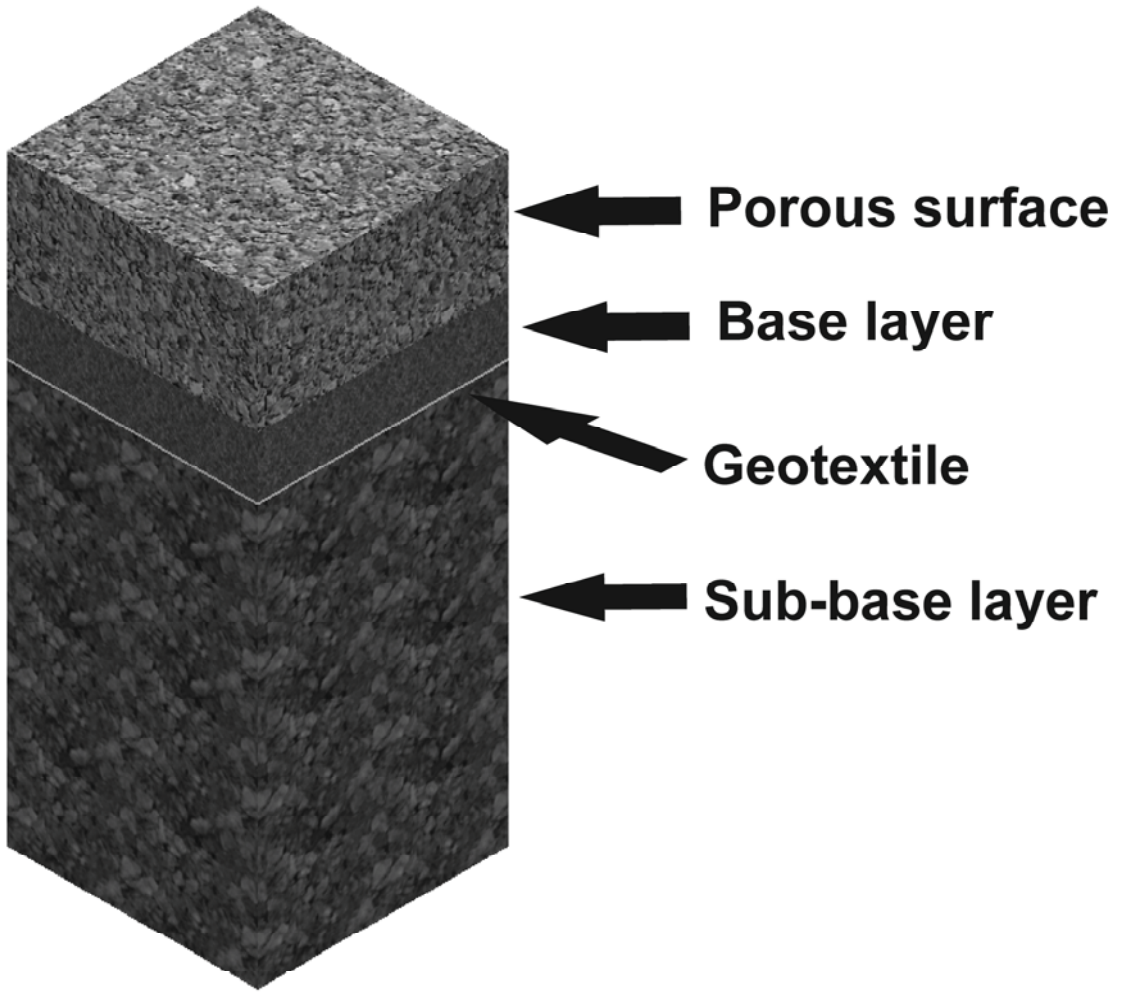


Figure 1.

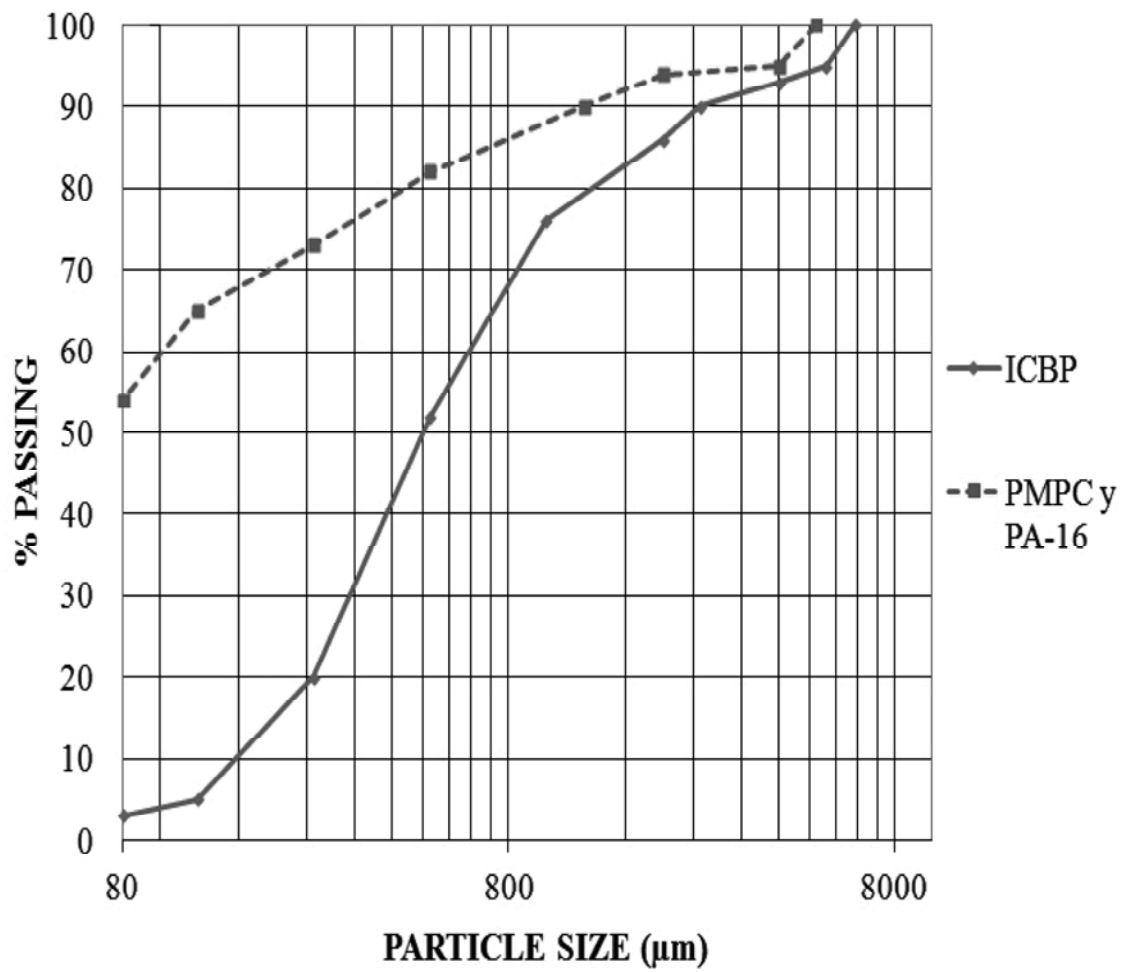
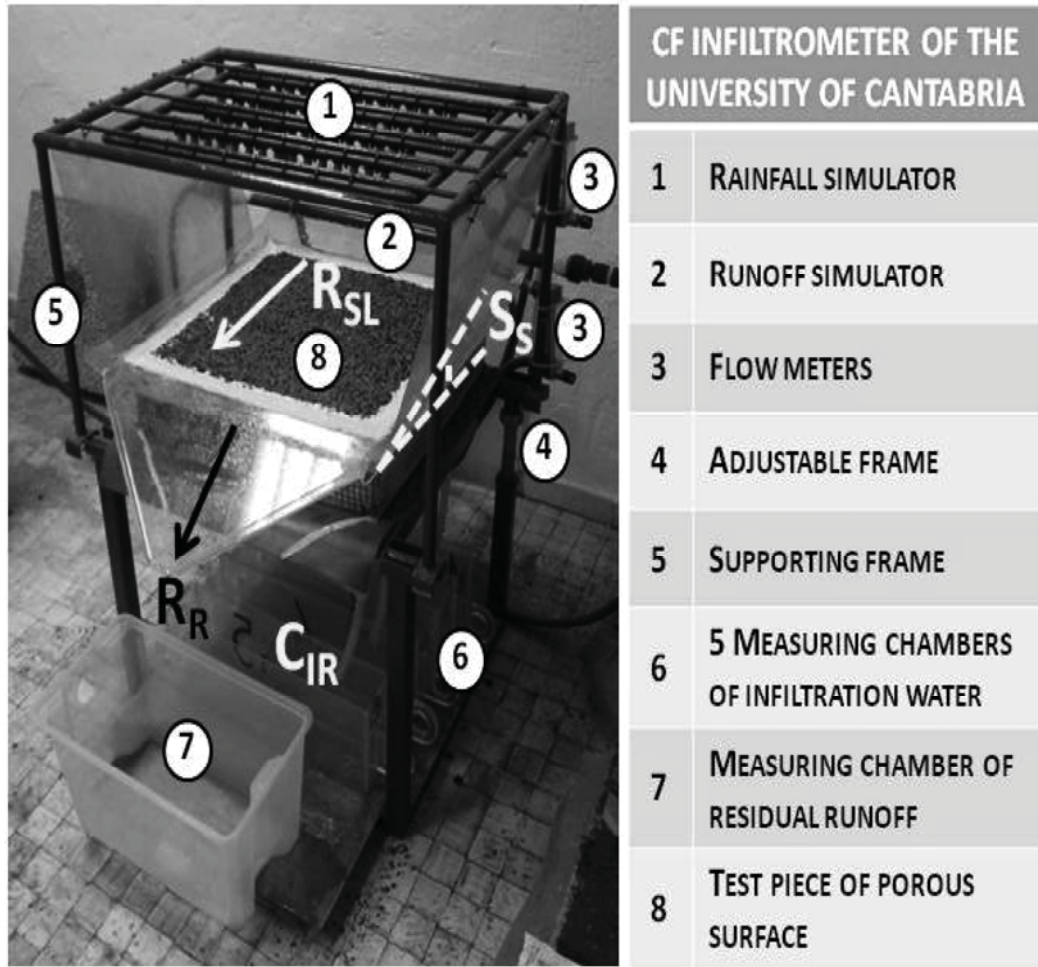


Figure 2.



CF INFILTRMETER OF THE UNIVERSITY OF CANTABRIA

1	RAINFALL SIMULATOR
2	RUNOFF SIMULATOR
3	FLOW METERS
4	ADJUSTABLE FRAME
5	SUPPORTING FRAME
6	5 MEASURING CHAMBERS OF INFILTRATION WATER
7	MEASURING CHAMBER OF RESIDUAL RUNOFF
8	TEST PIECE OF POROUS SURFACE

Figure 3.

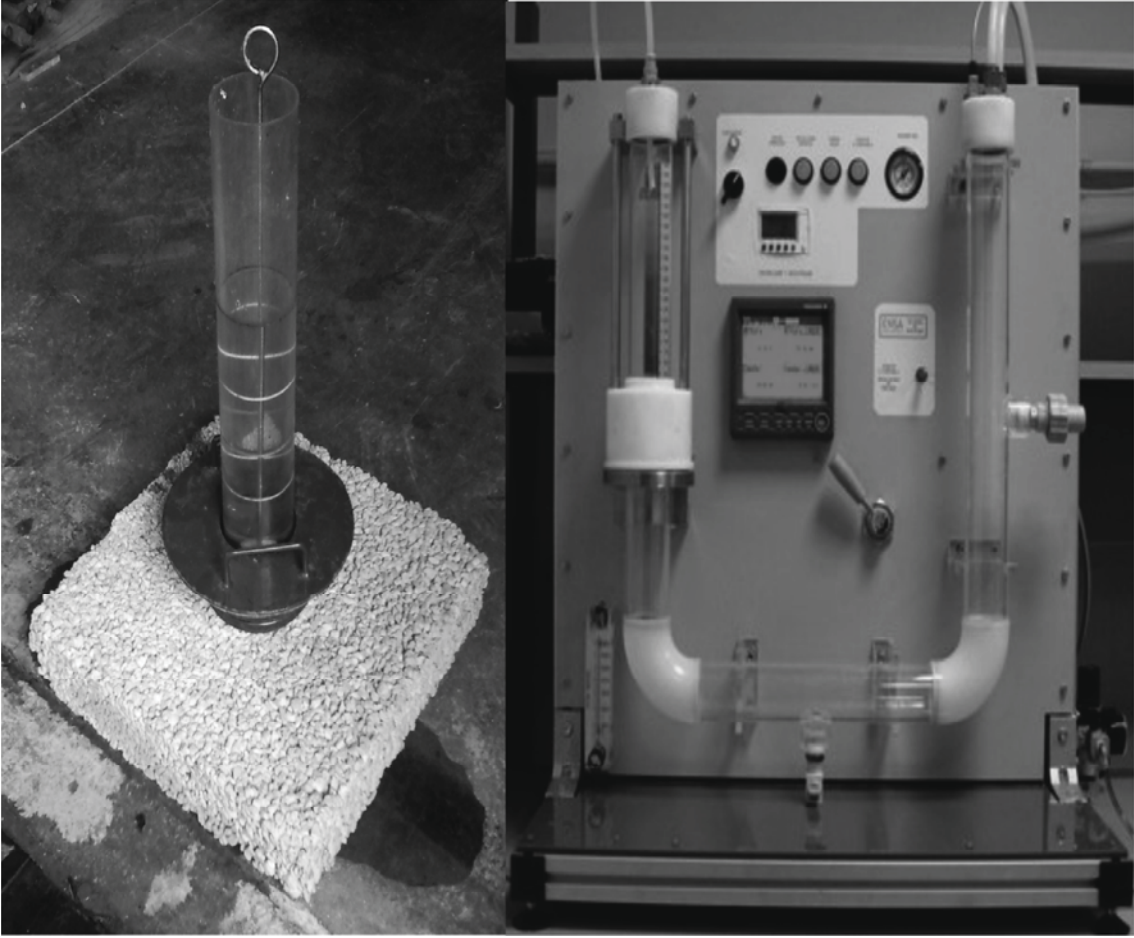


Figure 4.

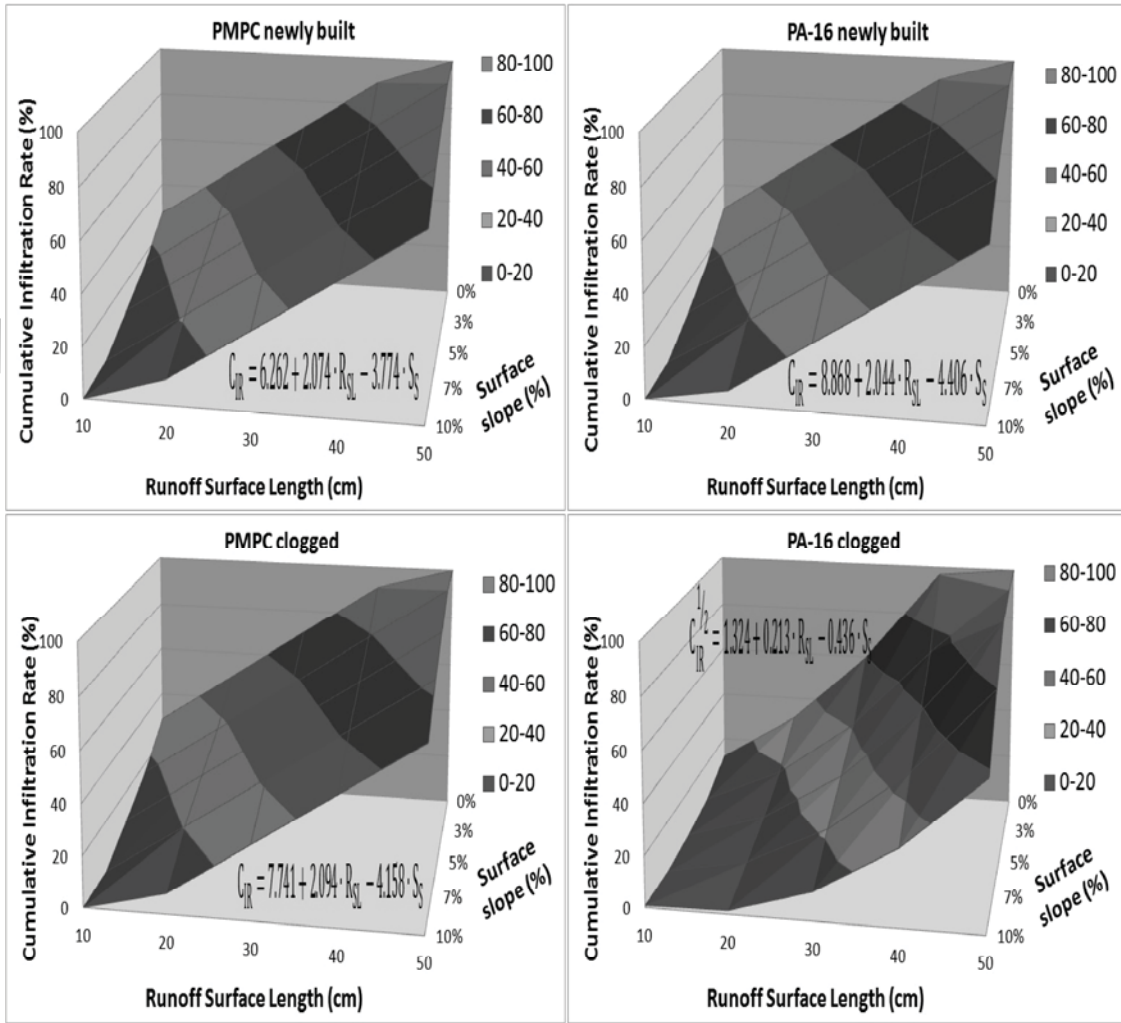


Figure 5.

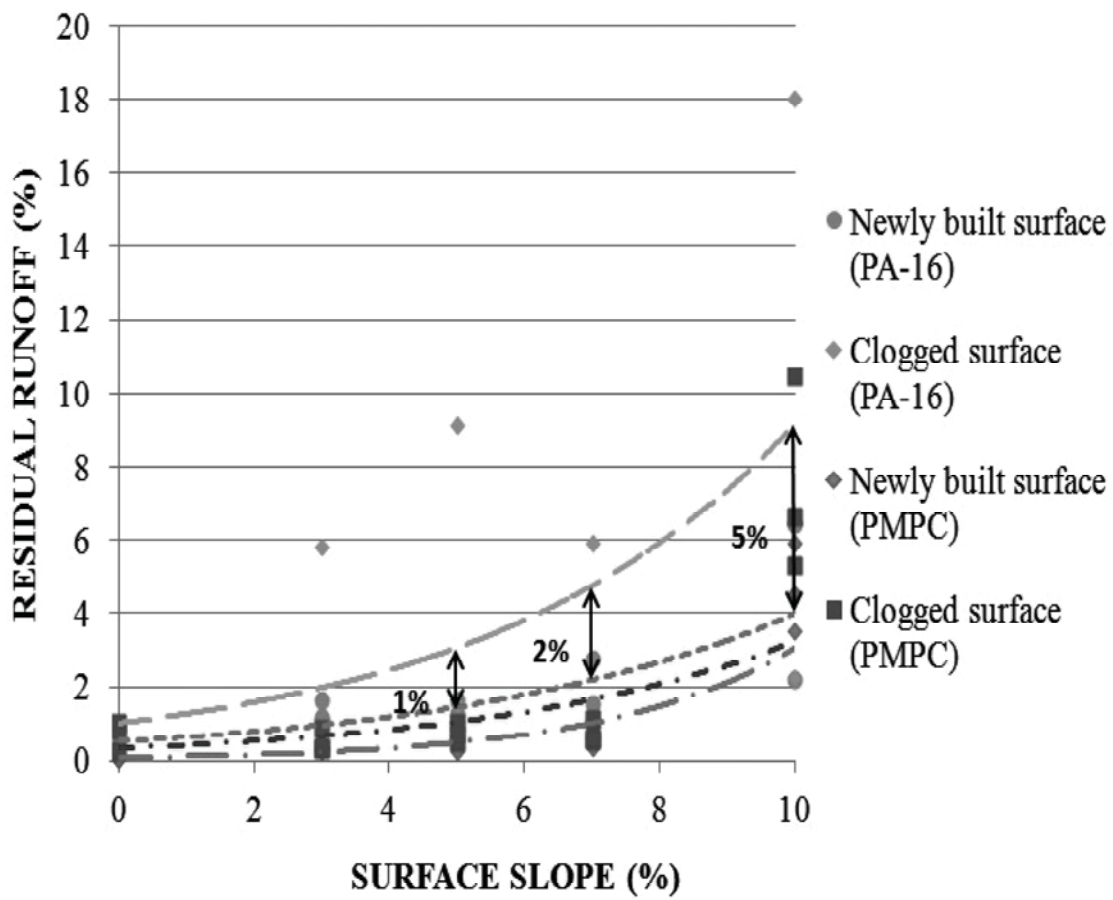


Figure 6.

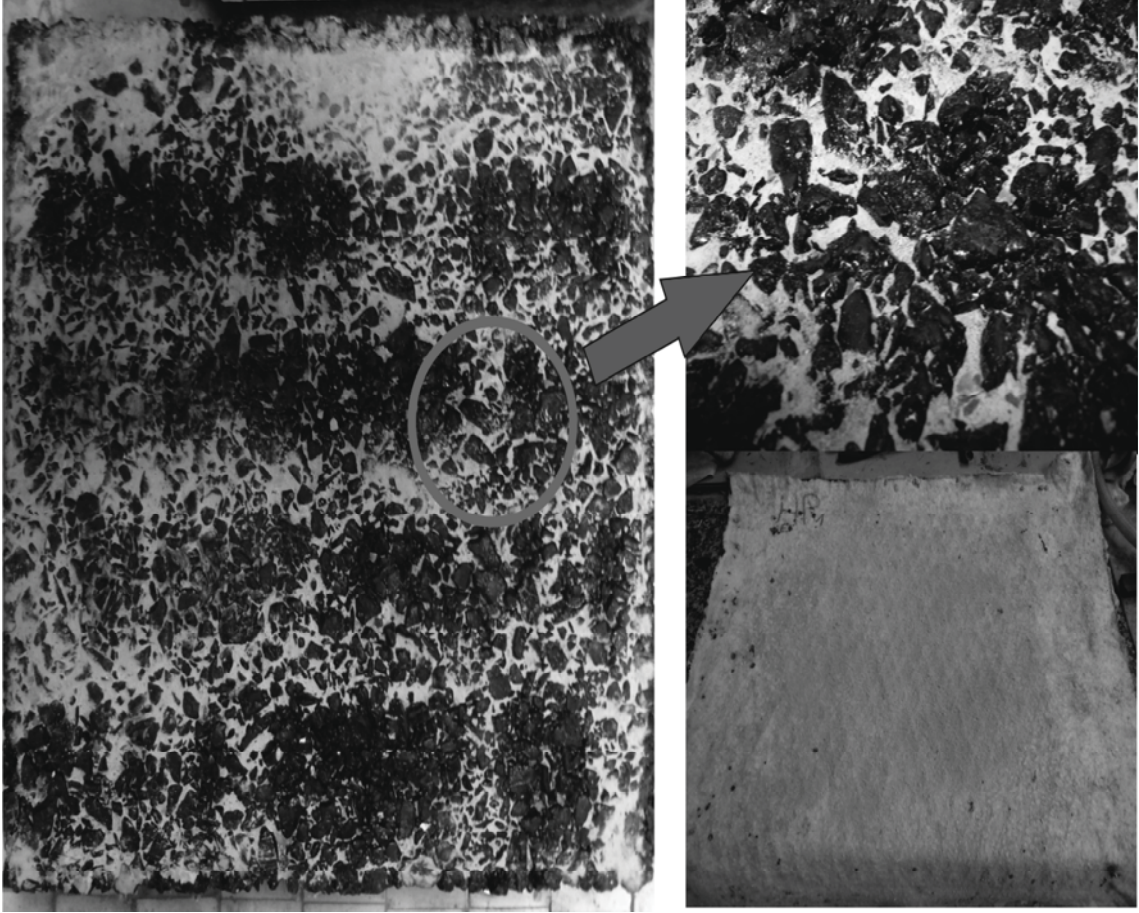


Figure 7.